AIAA SciTech Forum
23-27 January 2023, National Harbor, MD & Online
AIAA SCITECH 2023 Forum

10.2514/6.2023-2417

# Additively Manufactured Flexible Hybrid Electronic Sensor for Discrete Fatigue Crack Detection

Corinne A. Smith* and Austin R.J. Downey†
*University of South Carolina, Columbia, SC, 29208, United States*

**Additively manufactured flexible electronic sensors present new geometries for structural health monitoring applications. Conformable substrates can form sensing skins to provide a lightweight method of monitoring defects. A printed flexible hybrid electronic sensor is presented in this work that uses an array of digital inputs to discretely monitor crack progression by breaking along with the defect. Via generation methods with polyimide film and silver ink are explored to create vias with a resistance of 61.10 mΩ. Double-sided printing techniques and soldering are performed to fabricate the sensor with a commercial PCB printer. The digital input array as a sensing method is validated with a tear test, and a wireless microcontroller is integrated with the PFHE sensor to perform data transfer for real-time monitoring.**

Downloaded by Corinne Smith on January 19, 2023 | http://arc.aiaa.org | DOI: 10.2514/6.2023-2417

## I. Nomenclature

| | | |
|---|---|---|
| SHM | = | structural health monitoring |
| PFE | = | printed flexible electronic |
| PFHE | = | printed flexible hybrid electronic |
| IoT | = | Internet of Things |

## II. Introduction

Fatigue cracking is common in aluminum aircraft structures and must be properly monitored to avoid fatigue failures. The location of a crack, particularly its proximity to areas classified as critical by the engineers, determines the severity of the damage [1]. Aircraft operation often uses the damage tolerance approach to develop a comprehensive program of inspections to detect damage before it can affect flight safety. In this approach, the structure's ability to safely sustain defects such as fatigue cracks is used to estimate the extent of damage allowed before the structure's residual strength falls below an acceptable limit. This approach requires proper inspection of crack propagation zones to monitor damage growth [2]. Certain areas, such as fastener locations are especially susceptible to fatigue cracks and should be monitored before reaching a critical size to allow remedial intervention [3].

Structural health monitoring (SHM), including crack detection, poses particular challenges on aircraft structures. Sensing technology must adhere to strict design requirements due to the limitations on size, weight, and power. In particular, sensors must be large-scale, lightweight, and low-power in order to allow effective monitoring without increasing the aircraft's payload [4]. Several different sensing methods created for aircraft have been studied extensively, including acoustic emission [5], electromagnetic sensing arrays [6], the eddy current method [7], and strain modal analysis [8], among others.

Printed flexible electronics (PFEs) offer a simple method of creating sensing sheets, a type of sensing technology used for crack detection and characterization [9]. Printed flexible electronics are electronic devices that have been created through additively manufactured conductive lines onto stretchable or conformable substrates [10]. A large-area resistive strain sensing sheet developed by Aygun et al. consists of a two-dimensional thin-film resistive strain sensor array [11] and is fabricated using a flexible printed circuit board manufactured by Q-Flex Inc, which uses polyimide film as one of their flexible substrates [12]. A sensitive skin for crack monitoring on concrete bridges created by Zhou et al. [13] utilizes a flexible resin paper substrate with two independent layers of silk-screen printed conductive silver film. The sensitive skin detects damage when the crack opening causes a silver film to break. Through monitoring the conductivity of the silver film tracks, the sensitive skin localizes the crack area in a coordinate grid. A semi-decentralized network of

*Research Assistant, Department of Mechanical Engineering, 300 Main St. Columbia SC, 29208
†Assistant Professor, Department of Mechanical Engineering, 300 Main St. Columbia SC, 29208



Copyright © 2023 by the American Institute of Aeronautics and Astronautics, Inc. All rights reserved.

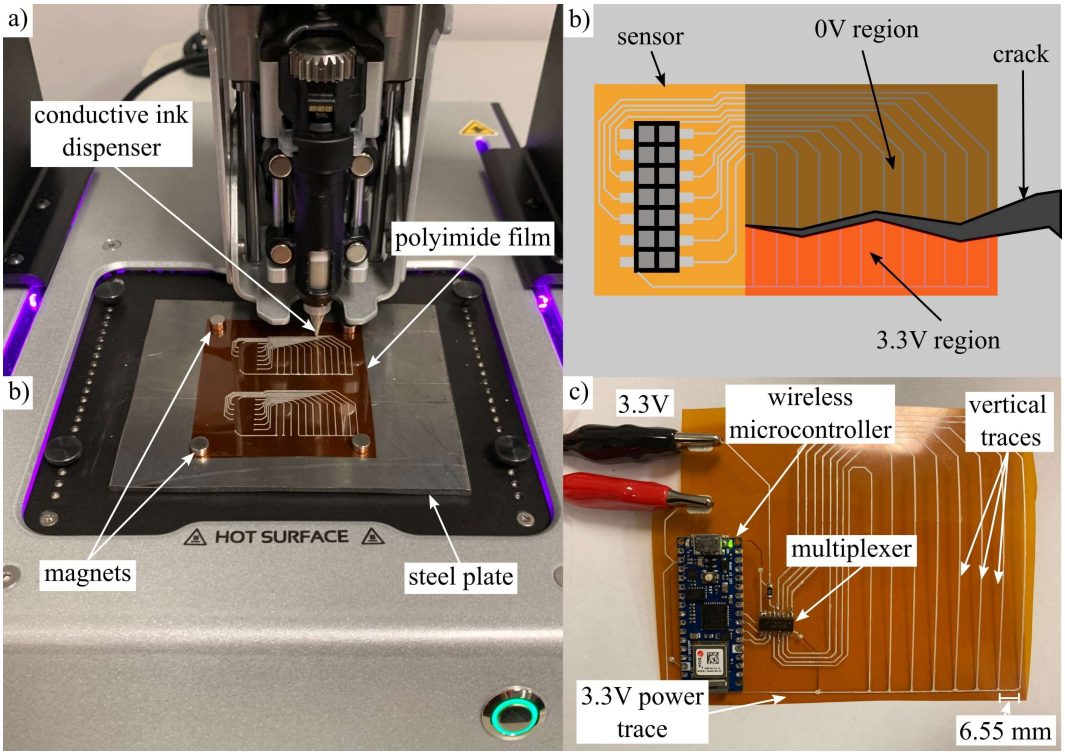


**Fig. 1 Sensor manufacturing showing a) the Voltera V-One printing conductive ink onto polyimide film to manufacture two modular PFE sensors; b) the working principle of the array of digital inputs, and; c) the self-contained PFHE sensor.**

PFE piezoelectric sensors presented by Wang et al. [14] form a wired sparse sensor network for pipe damage detection. The piezoelectric wafer is encapsulated in a polyimide film and data is transmitted to a post-processing center based on the NI PXI platform, allowing fewer sensors to be deployed for a large area, but still requiring a wired connection to process data.

This work focuses on the manufacturing process for novel printed flexible electronic and printed flexible hybrid electronic crack detection sensors. Two sensors are presented: a modular one-dimensional PFE sensor and a self-contained one-dimensional printed hybrid flexible electronic (PFHE) sensor. Both of these allow different approaches to creating a lightweight, decentralized network of crack-monitoring flexible sensors. Additive manufacturing permits prototypes to be made quickly and on-site, and allows design possibilities that go beyond a stand-alone sensor. The modular one-dimensional PFE sensor presented displays the sensing principle of a one-dimensional array of digital inputs to monitor crack progression. This sensor is used in a tear test to demonstrate the effectiveness of this geometry in detecting cracks and estimating their length in the x-direction. PFHEs are a type of PFE that include semiconductor devices to expand the capabilities of PFEs beyond just conductive traces [10]. The one-dimensional PFHE sensor elevates the modular PFE sensor by integrating a multiplexer and wireless microcontroller to allow monitoring via the Internet of Things (IoT). Like the modular prototype sensor, the one-dimensional PFHE sensor measures crack progression in the x-direction only. The contributions of this work are as follow: 1) a via generation technique for polyimide film, 2) a manufacturing process for silver ink polyimide PFHEs compatible with a commercial PCB printer, 3) a tear test to validate the digital input array sensing technique for monitoring cracks.

## III. Sensor Design and Fabrication

Figure 1 shows the PFE sensor's manufacturing process and sensing principle, along with the fabricated PFHE sensor. Both are printed using a Voltera V-One PCB printer, which is a consumer-grade electronics additive manufacturing system. It is advertised as being used with traditional printed circuit boards but has been adapted for this sensor to print conductive ink onto polyimide film, a flexible substrate commonly used in PFEs. The V-One allows custom printing for



Downloaded by Corinne Smith on January 19, 2023 | http://arc.aiaa.org | DOI: 10.2514/6.2023-2417

both PFEs and PFHEs, with a soldering feature built-in for semiconductor components. The sensors presented were created using V-One's conductive ink for the vertical traces and solder for the connections.

### A. Sensing Principle

The modular PFE sensor is designed to provide a discrete measure of crack progression. A series of traces perpendicular to the crack are broken as the crack progresses, indicating the crack's length in the x-direction. The bottom trace is given a voltage of 3.3 V, elevating each trace to a digital high and creating an array of digital inputs that can be read by an external microcontroller. As a crack breaks the vertical traces, the distal end of the trace which is connected to the output port will drop to 0 V as it is no longer continuous with the 3.3 V bottom trace. This change in voltage can be detected and the broken trace corresponded to a distance.

The PFE sensor can be improved by adding semiconductor components on-device. The current modular design requires a bulky and fragile connector to a rigid microcontroller, which is not ideal for flexible structural health monitoring applications. In the one-dimensional PFHE sensor, the sensing plane is conserved from the modular PFE sensor and integrated with a microcontroller for onboard computing. Microcontroller integration requires more complex manufacturing techniques, such as via generation, double-sided printing, and soldering.

Downloaded by Corinne Smith on January 19, 2023 | http://arc.aiaa.org | DOI: 10.2514/6.2023-2417

### B. Via Generation

Vias are required as the electronic print complexity increases, resulting in crossing traces that must be manufactured with double-sided printing. This is a common issue in additively manufactured flexible electronics. One method explored by Ta et al [15] inserts a metal body between layers to create the connection, such as a staple. This method is limited by via location and size and is not suitable for flexible applications due to the large and rigid structure of the metal body. A more effective method they explored creates a hole in the substrate using either a drill bit, felting needle, or hole punch, and fills the hole with silver nanoparticle ink. This method was expanded on by Jansson et al [16], which investigated the optimal sequence for via manufacture on a TPU substrate. The paper explored different sequences of drilling and printing on the front and back sides of the substrate to determine which created the lowest resistance and found that the process configuration was highly dependent on the application. As neither of these studies used a polyimide substrate, via testing was conducted using the Voltera's setup to determine ideal cutting methods and process configurations for the PFHEs.

Drilling and $CO_2$ laser cutting were the two cutting methods tested, as the Voltera comes with a small drill and polyimide can be transformed into conductive graphene with the use of a 405 nm $CO_2$ laser [17]. Four different via generation processes were tested to determine which via produced the lowest resistance as compared to rigid copper vias, which had a measured resistance of 8.30 m$\Omega$. Process 1 first printed a conductive ink electrode on the front side and then used the $CO_2$ laser to create a hole from the front side before a back electrode was printed. Process 2 first printed a conductive ink electrode on the front side before using a 1 mm drill bit to create a hole from the front side into the back, where the back electrode was printed. Process 3 first creates the hole with the $CO_2$ laser on the front side before printing the front and then back electrodes. Process 4 first drills the hole with the 1 mm drill bit on the front side before printing the front and back electrodes. Three samples of each process were manufactured using the Voltera and the resistance of each via was measured using a BK Precision 2841 DC resistance meter. Figure 2 shows the via test setup and process diagrams.

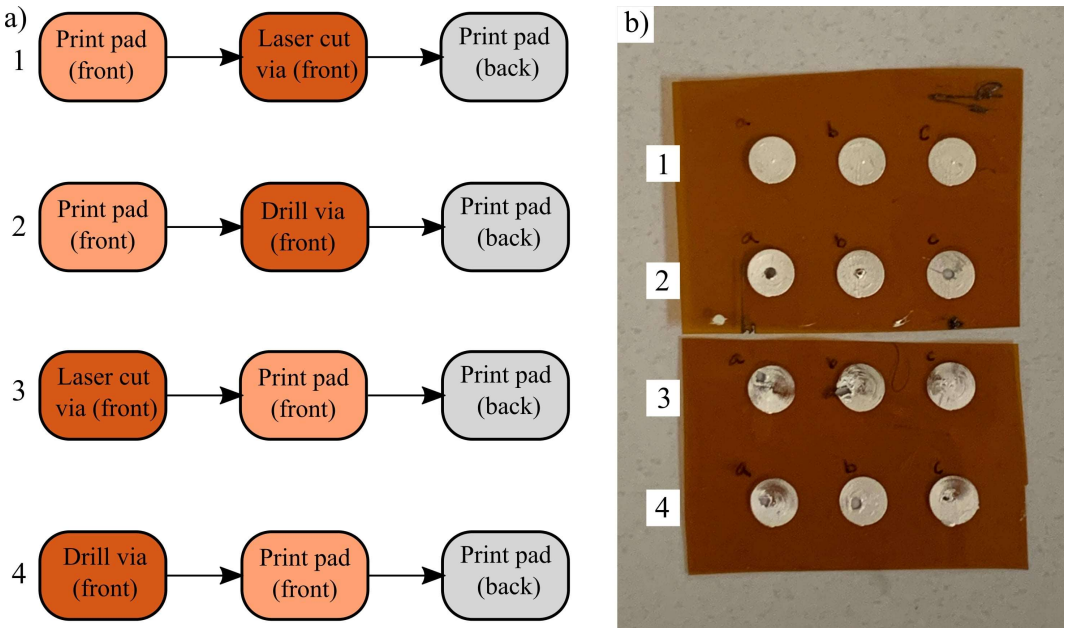


**Fig. 2 Via generation processes showing a) process flow and b) printed test samples.**

The resistance for each sample was measured and an average for each process was calculated and is displayed in Figure 3. Process 1 had the highest resistance that exceeded the range of the resistance meter, as the laser was unable to cut through the silver ink electrode due to its differing chemistry from polyimide. Process 2 had the lowest resistances of 55.84 and 61.10 mΩ before and after buffing, making it the ideal via generation process. It was also considerably easier to drill through the silver electrode as opposed to the plain polyimide in process 4, which had resistances of 108.53 and 90.79 mΩ, as the electrode provides some stability for the drill and does not get caught during the retraction. Process 3 produced much higher resistances of 260.94 and 536.66 mΩ compared to processes 2 and 4, which increased after buffing. It is believed that the force of buffing caused graphene generated by the laser to be broken off from the substrate, accounting for the higher resistance. Process 4 produced results comparable to process 2, but its increased manufacturing difficulty makes process 2 the best via generation process.

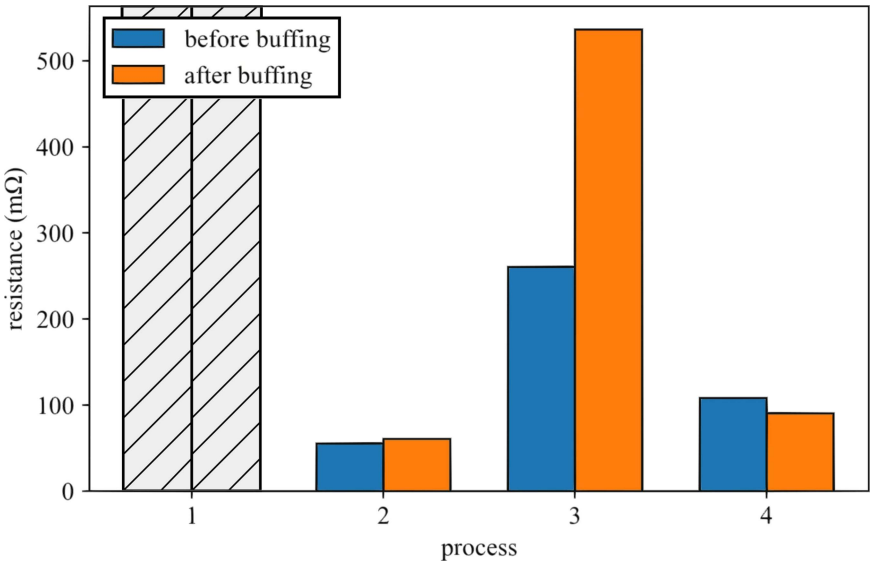


**Fig. 3 Average experimental resistance of vias for processes 1-4 before and after mechanical buffing. Process 1 has a resistance exceeding the meter's maximum for both values.**



Downloaded by Corinne Smith on January 19, 2023 | http://arc.aiaa.org | DOI: 10.2514/6.2023-2417

### C. Sensor manufacture

The manufacturing process for the one-dimensional PFHE is more complex than that of the prototype sensor as it requires printing on both sides of the substrate due to the placement of the multiplexer. Via generation and soldering are also required, further increasing complexity. These processes provide novel challenges with the manufacturability of the sensors using the Voltera, which is intended for rigid PCBs. To overcome these challenges, a manufacturing process was developed and is outlined in figure 4.

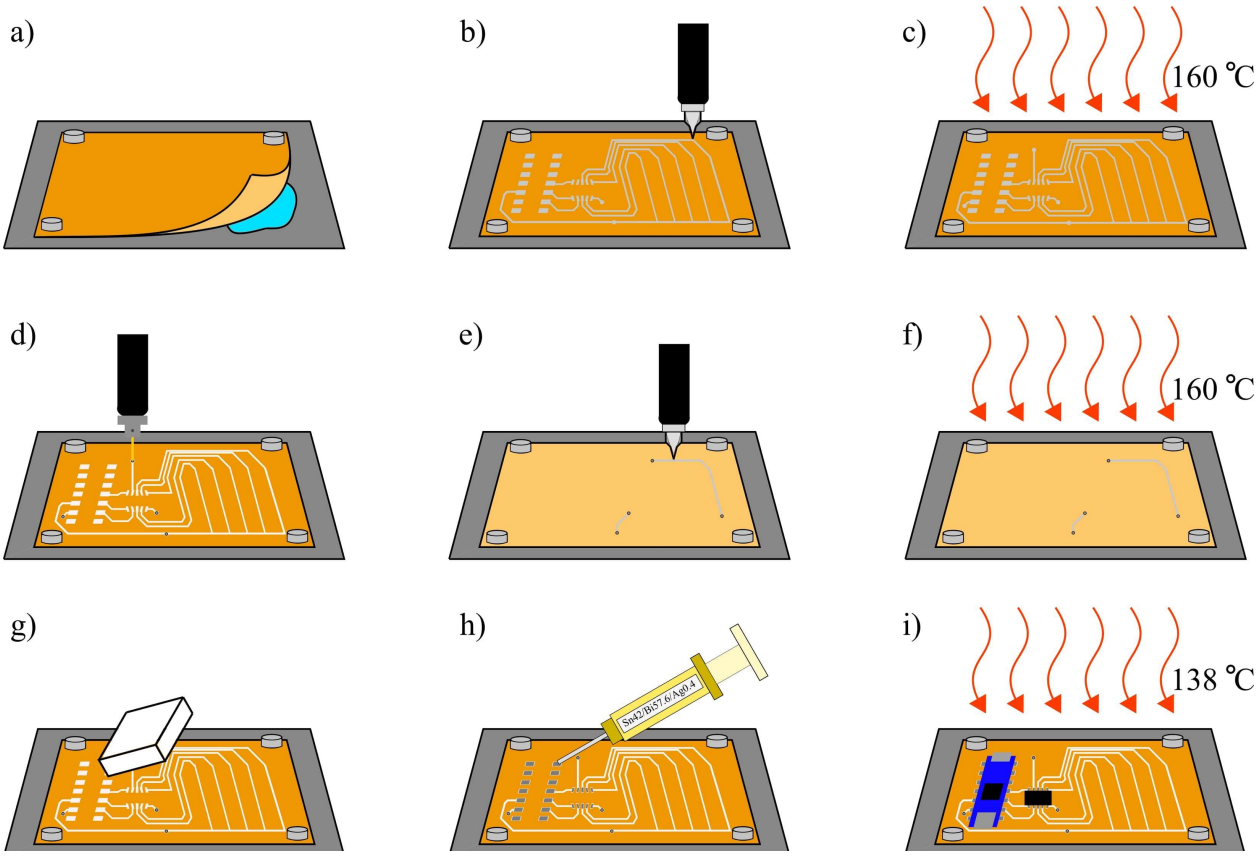


**Fig. 4 Double layer manufacturing process for one-dimensional PFHE sensor. From left to right: a) substrate plate adherence; b) front layer print; c) front layer thermal sintering; d) front layer via generation; e) back layer print; f) back layer thermal sintering; g) buffing; h) solder paste application; and i) solder reflow.**

The manufacturing process begins with adhering the polyimide substrate to the metal build plate with a combination of button magnets and isopropyl alcohol. Due to the size of the substrate, isopropyl is used to induce adhesion between the base plate and polyimide and create a flatter surface that discourages bulging in the center without disturbing the print surface area. Magnets are used as reinforcement on the corners out of the print zone. Once adhered, the Gerber file of the front copper layer, which is generated in electronic design automation software, is uploaded to the Voltera and converted into G-code. The G-code is run and the design is printed with the Voltera's Flex 2 flexible conductive ink. Once the ink is printed, it is thermally sintered at 160°C for 48 minutes to maximize conductivity. After curing, process 2 via generation is executed and 0.70 mm holes are drilled on the front side of the via. Before drilling, a sacrificial layer is added underneath the substrate to avoid drilling into the base plate. The areas where vias are drilled have a 1.3 mm diameter front electrode to ensure there is enough ink left after drilling for traces to connect to. After drilling, the substrate is flipped and the Gerber file for the back copper layer is uploaded and printed. After printing, thermal sintering on the back layer must be performed for 48 minutes to set the ink. Once all ink is set, the pads that will be soldered must be prepped by mechanically buffing the area to remove the outer layer of ink. This process ensures a more complete solder wetting by ensuring contact with fully sintered ink. Sn42/Bi57.6/Ag0.4 solder paste is then dispensed on the pads and the components are placed on their footprints, either manually or with a pick-and-place

Downloaded by Corinne Smith on January 19, 2023 | http://arc.aiaa.org | DOI: 10.2514/6.2023-2417

machine. Sn42/Bi57.6/Ag0.4 solder paste is used due to its lower melting temperature at 138°C, which prevents damage to the printed ink pads. Finally, the Voltera reflow solders components for 28 minutes, using a heating curve suitable for the chemistry of the paste.

Important considerations during the manufacturing process include the surface plane alignment, ink dispensing finish, drill retract height, and reflow contact. The surface plane must be very flat to evenly print ink and avoid dry spots, which occur when the ink nozzle becomes too close to the substrate that ink cannot properly dispense. This can be addressed by using the screw holes on the Voltera printer bed to clamp down the base plate, as well as by using the combination of button magnets and isopropyl to secure the substrate. Ink dispensing must be monitored to avoid dry spots and reduce the number of reprints. The nozzle flow and height can be adjusted to account for an uneven substrate and provide more tolerance between the tip and print surface. It was found that increasing the nozzle z-axis from 10 mm to 13 mm greatly improved the ink dispensing finish. Drilling through polyimide causes the substrate to be pulled up slightly with the drill during retraction, so the drill retraction height must be adjusted from 0.1 mm to at least 3.0 mm to avoid tearing the substrate. The reflow process requires good contact between the metal base plate and the substrate to melt the solder due to its low melting point. This can be ensured by adjusting the magnets closer to the components to avoid bulging.

The major limitation of the manufacturing process is the time, particularly with the thermal sintering (48 minutes) and the solder reflow (28 minutes). Printing is a relatively quick process in comparison, consuming on average 12 minutes for the front print and 2 minutes for the back print. As the sintering is a heating process that does not require the Voltera's G-code or dispensing functionalities, one way to accelerate the process would be to have a separate apparatus just for sintering so that the Voltera can be used to print multiple sensors simultaneously.

Downloaded by Corinne Smith on January 19, 2023 | http://arc.aiaa.org | DOI: 10.2514/6.2023-2417

## IV. Experimental Validation

To validate the sensor's ability to detect crack lengthening, the sensor was subjected to a tear test using an aluminum sample. The sensor was adhered to a small sheet of aluminum with a 19 mm cut to simulate an initialized fatigue crack. The farthest vertical trace (trace 12) was situated perpendicular to the cut so that the crack would progress horizontally toward the innermost vertical trace (trace 1). The sensor was connected to an Arduino Mega, with each trace corresponding to a digital input. The Arduino Mega continuously sampled the voltage of each digital input and recorded the pin state, so that a broken trace would change from a state of 1 to a state of 0. The aluminum sample was slowly torn apart using a material testing system as shown in figure 5.

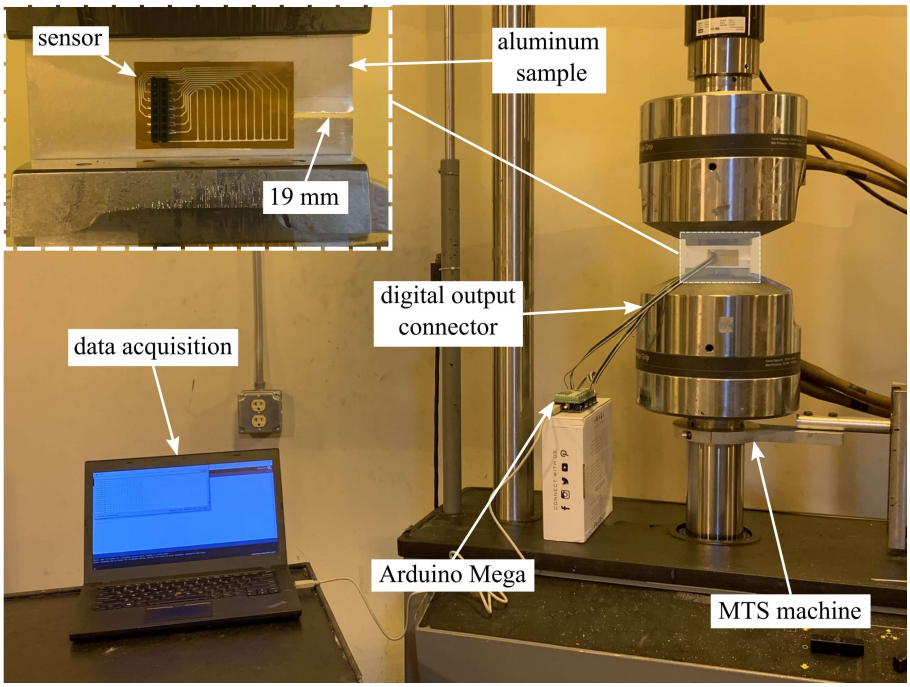


**Fig. 5 Experimental setup for tear test using prototype sensor.**

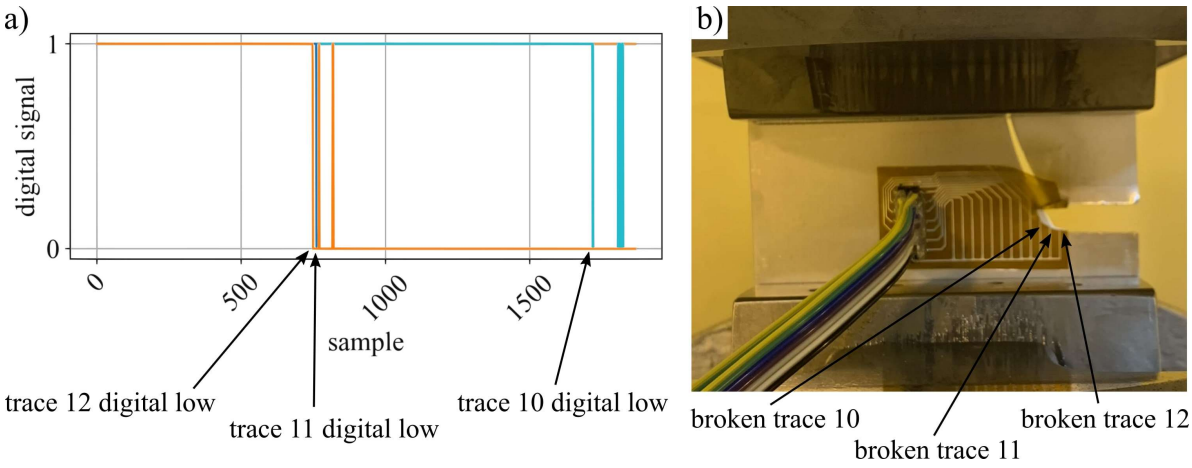


**Fig. 6 Aftermath of the tear test experiment showing a) plotted data from all 12 digital inputs and b) the torn specimen.**

Figure 6 shows the results of the tear test. Traces 12, 11, and 10 were broken as the crack progressed while the subsequent traces remained intact. The plot shows that the digital output dropped from high to low for each trace and settled after varying periods of time. Traces 12 and 11 were broken quickly after one another while traces 11 and 10 were allotted more time in between breaks, demonstrating that the prototype sensor is effective in detecting both sudden and slow changes in crack length. Initial breaking gives an unsteady signal, as demonstrated by the jumping between a digital high and low for traces 11 and 10, but settles after a few seconds, maintaining reading accuracy after breaking.

The wireless capabilities of the one-dimensional PFHE sensor were tested to determine if the sensor could act as a self-contained wireless node. As the sensing principle was validated by the prototype sensor, the same digital input array was adopted by the one-dimensional PFHE sensor and integrated with an 8-channel multiplexer and a wireless microcontroller. The microcontroller sweeps through the multiplexer to read each input and sends data to the GUI via WiFi to monitor each line, which are spaced 6.55 mm apart. A serial connection can also be established to monitor data. In this experiment, the microcontroller was programmed to periodically send the array of digital inputs to the GUI to validate the data transfer capabilities and quality for the flexible printed substrate.

The sensor is able to send accurate data with no apparent interruption due to the flexible materials. As no lines have been broken, all digital inputs in the array should read 1, which is validated by the serial monitor output. The GUI displays values that have been transmitted wirelessly for channels 0-4, proving the sensor's ability to perform data transfer. The experiment was performed using a breadboard of the circuit and the data were consistent and transferred at similar rates. However, the power draw for the one-dimensional PFHE on polyimide was between 198 mW and 264 mW, while the power draw for the breadboarded sensor was between 66 and 165 mW. This is likely due to the difference in electrical conductivity between the copper and silver ink traces. Because the silver ink sensor consumes almost double the power of the copper version, the power supply will be a prominent issue in the design of PFHE sensors for aircraft applications.

## V. Conclusion

The sensing and manufacturing techniques described in this paper are effective in monitoring crack progression. The one-dimensional PFE sensor demonstrated through a tear test the capability of using an array of digital inputs to discretely monitor the progression of a crack in the x-direction. For more complex, double-sided designs, via testing showed the most effective via generation technique for a polyimide substrate to be printing the front electrode, drilling through the substrate, then printing the back electrode. This process resulted in a resistance of 61.10 mΩ, which is 7.36 times higher than that of copper. The manufacturing process outlined in this work detailed the steps to create the one-dimensional PFHE sensor, beginning from substrate adherence to the build plate and ending with soldering. The process has shown to be minimal and integrated easily with the Voltera to automate most of the manufacturing and produced working sensors. To improve the usability of the one-dimensional PFE sensor design, the one-dimensional PFHE sensor demonstrated a straightforward wireless microcontroller integration that allows the sensor to be self-contained and useful in real-time structural health monitoring.



Downloaded by Corinne Smith on January 19, 2023 | http://arc.aiaa.org | DOI: 10.2514/6.2023-2417

Future work will focus on adding another dimension to the PFHE to monitor crack progression in the y-direction as well as the x-direction. The via generation and manufacturing techniques discussed in this work can be used to create a second array of digital inputs on the back of the substrate to facilitate this. Wider area sensors may be generated by using a different printer with a larger base plate, and the steps discussed here for manufacturing conductive ink sensors on polyimide can be applied. One difficulty to be addressed in the future include sensor resolution, as the distance between sensing lines is limited by the number of digital inputs on the multiplexer. More inputs require a larger multiplexer, which is a rigid component that will reduce the flexibility of the sensing node. Another difficulty is the power supply, as the one-dimensional PFHE sensor was found to draw twice the power of its breadboard equivalent.

## Acknowledgments

This research is supported by the Federal Highway Administration (FHWA) Transportation Pooled Fund Study, TPF-5(449), jointly sponsored by the Departments of Transportation of Iowa, Kansas, South Carolina, and North Carolina.

Downloaded by Corinne Smith on January 19, 2023 | http://arc.aiaa.org | DOI: 10.2514/6.2023-2417

## References

[1] Greenemeier, L., "What Causes an Airline Fuselage to Rupture Mid-Flight? How Can This Be Prevented?" *Scientific American*, 2011. URL https://www.scientificamerican.com/article/southwest-airplane-aluminum-cracks/.

[2] Shanyavskiy, A. A., Soldatenkov, A. P., and Toushentsov, A. A., "Foundation of damage tolerance principles in-service for the RRJ-95 aircraft structural components," *Fatigue and Fracture of Engineering Materials and Structures*, 2021. https://doi.org/10.1111/ffe.13478.

[3] Underhill, P. R., and Krause, T. W., "Crack Detection Around Raised Head Rivets in Aluminum Aircraft Structures," *Journal of Nondestructive Evaluation*, Vol. 40, 2021. https://doi.org/10.1007/s10921-021-00826-1.

[4] Wang, Y., Hu, S., Xiong, T., Huang, Y., and Qiu, L., "Recent progress in aircraft smart skin for structural health monitoring," *Structural Health Monitoring*, Vol. 0, No. 0, 2021, p. 14759217211056831. https://doi.org/10.1177/14759217211056831, URL https://doi.org/10.1177/14759217211056831.

[5] Karimian, S. F., Modarres, M., and Bruck, H. A., "A new method for detecting fatigue crack initiation in aluminum alloy using acoustic emission waveform information entropy," *Engineering Fracture Mechanics*, Vol. 223, 2020, p. 106771. https://doi.org/https://doi.org/10.1016/j.engfracmech.2019.106771, URL https://www.sciencedirect.com/science/article/pii/S0013794419308896.

[6] Steigmann, R., Iftimie, N., Dobrescu, G. S., Danila, A., Barsanescu, P. D., Stanciu, M. D., and Savin, A., "Fatigue cracks in aluminum alloys structures detection using electromagnetic sensors array," *IOP Conference Series: Materials Science and Engineering*, Vol. 997, No. 1, 2020, p. 012031. https://doi.org/10.1088/1757-899x/997/1/012031, URL https://doi.org/10.1088/1757-899x/997/1/012031.

[7] Bohacova, M., "Methodology of short fatigue crack detection by the eddy current method in a multi-layered metal aircraft structure," *Engineering Failure Analysis*, Vol. 35, 2013, pp. 597–608. https://doi.org/https://doi.org/10.1016/j.engfailanal.2013.06.009, URL https://www.sciencedirect.com/science/article/pii/S1350630713002094, special issue on ICEFA V- Part 1.

[8] Khatir, S., Abdel Wahab, M., Boutchicha, D., and Khatir, T., "Structural health monitoring using modal strain energy damage indicator coupled with teaching-learning-based optimization algorithm and isogoemetric analysis," *Journal of Sound and Vibration*, Vol. 448, 2019, pp. 230–246. https://doi.org/https://doi.org/10.1016/j.jsv.2019.02.017, URL https://www.sciencedirect.com/science/article/pii/S0022460X19301087.

[9] Yao, Y., Tung, S.-T. E., and Glisic, B., "Crack detection and characterization techniques—An overview," *Structural Control and Health Monitoring*, Vol. 21, No. 12, 2014, pp. 1387–1413. https://doi.org/https://doi.org/10.1002/stc.1655, URL https://onlinelibrary.wiley.com/doi/abs/10.1002/stc.1655.

[10] NextFlex, "About Flexible Hybrid Electronics: Defining Flexible Hybrid Electronics (FHE)," , 2022. URL https://www.nextflex.us/about/about-fhe/.

[11] Aygun, L. E., Kumar, V., Weaver, C., Gerber, M., Wagner, S., Verma, N., Glisic, B., and Sturm, J. C., "Large-Area Resistive Strain Sensing Sheet forStructural Health Monitoring," *Sensors (Basel)*, 2020. https://doi.org/10.3390/s20051386.

[12] Q-FlexInc., "Technology," Online, 2022. URL https://www.qflexinc.com/technology/.

[13] Zhou, Z., Zhang, B., Xia, K., Li, X., Yan, G., and Zhang, K., "Smart film for crack monitoring of concrete bridges," *Structural Health Monitoring*, Vol. 10, No. 3, 2011, pp. 275–289. https://doi.org/10.1177/1475921710373288, URL https://doi.org/10.1177/1475921710373288.

[14] Wang, Q., Hong, M., and Su, Z., "A sparse sensor network topologized for cylindrical wave-based identification of damage in pipeline structures," *Smart Materials and Structures*, Vol. 25, No. 7, 2016. https://doi.org/10.1088/0964-1726/25/7/075015, URL https://iopscience.iop.org/article/10.1088/0964-1726/25/7/075015/meta.

[15] Ta, T., Fukumoto, M., Narumi, K., Shino, S., Kawahara, Y., and Asami, T., "Interconnection and Double Layer for Flexible Electronic Circuit with Instant Inkjet Circuits," *Proceedings of the 2015 ACM International Joint Conference on Pervasive and Ubiquitous Computing*, Association for Computing Machinery, New York, NY, USA, 2015, p. 181–190. https://doi.org/10.1145/2750858.2804276, URL https://doi.org/10.1145/2750858.2804276.

[16] Jansson, E., Korhonen, A., Hietala, M., and Kololuoma, T., "Development of a full roll-to-roll manufacturing process of through-substrate vias with stretchable substrates enabling double-sided wearable electronics," *International Journal of Additive Manufacturing Technology*, Vol. 111, 2020, pp. 3017–3027. https://doi.org/https://doi.org/10.1007/s00170-020-06324-4.

[17] Ye, R., James, D. K., and Tour, J. M., "Laser-Induced Graphene: From Discovery to Translation," *Advanced Materials*, Vol. 31, No. 1, 2019, p. 1803621. https://doi.org/https://doi.org/10.1002/adma.201803621, URL https://onlinelibrary.wiley.com/doi/abs/10.1002/adma.201803621.

Downloaded by Corinne Smith on January 19, 2023 | http://arc.aiaa.org | DOI: 10.2514/6.2023-2417